ESC European Society of Cardiology

European Heart Journal - Cardiovascular Imaging (2017) **00**, 1–9
doi:10.1093/ehjci/jex309

Comparison of MOLLI, shMOLLLI, and SASHA in discrimination between health and disease and relationship with histologically derived collagen volume fraction

Nicholas Child[1,2], Gonca Suna[2,3], Darius Dabir[1,4], May-Lin Yap[1], Toby Rogers[1,3], Misha Kathirgamanathan[1], Eduardo Arroyo-Ucar[1,5], Rocio Hinojar[1], Islam Mahmoud[1], Christopher Young[6], Olaf Wendler[7], Manuel Mayr[2], Banher Sandhu[1], Geraint Morton[8], Marion Muhly-Reinholz[9], Stefanie Dimmeler[9], Eike Nagel[1,10], and Valentina O. Puntmann[1,10,11]*

[1]Department of Cardiology, Guys and St Thomas' NHS Trust, Westminster Bridge Road, London, UK; [2]Cardiovascular Division, King's College London, The Rayne Institute. St Thomas' Hospital, Westminster Bridge Road, London SE5 9RS, UK; [3]Department of Cardiology, King's College Hospital NHS Trust, Denmark Hill, London, UK; [4]Department of Radiology, University of Bonn, Regina-Pacis-Weg 3, Bonn, Germany; [5]Department of Cardiology, University of Hospital, Paseo de la Castellana, La Paz, Madrid, Spain; [6]Department of Cardiothoracic Surgery, Queen Alexandra Hospital, Guys and St Thomas' NHS Trust, Westminster Bridge Road, London, UK; [7]Department of Cardiothoracic Surgery, King's College Hospital, Denmark Hill, London, UK; [8]Department of Cardiology, Portsmouth Hospitals NHS Trust, Southwick Hill Road, Portsmouth, UK; [9]Institute for Cardiovascular Regeneration, University of Frankfurt, German Centre of Cardiovascular Research, (DZHK), Theodor-Stern-Kai 7, Frankfurt, Germany; [10]Institute of Experimental and Translational Cardiovascular Imaging, Goethe University Hospital Frankfurt, German Centre of Cardiovascular Research, (DZHK), Theodor-Stern-Kai 7, Frankfurt, Germany; and [11]Department of Cardiology, Goethe University Hospital Frankfurt, German Centre of Cardiovascular Research, (DZHK), Theodor-Stern-Kai 7, Frankfurt, Germany

Received 25 June 2017; editorial decision 30 October 2017; accepted 31 October 2017

Aims To determine the bioequivalence of several T1 mapping sequences in myocardial characterization of diffuse myocardial fibrosis.

Methods and results We performed an intra-individual sequence comparison of three types of T1 mapping sequences [MOdified Look-Locker Inversion recovery (MOLLI), Shortened MOdified Look-Locker Inversion recovery ((sh)MOLLI), and SAturation recovery single-SHot Acquisition (SASHA)]. We employed two model diseases of diffuse interstitial fibrosis [patients with non-ischaemic dilated cardiomyopathy (NIDCM), $n = 32$] and aortic stenosis [(AS), $n = 25$)]. Twenty-six healthy individuals served as controls. Relationship with collagen volume fraction (CVF) was assessed using endomyocardial biopsies (EMB) intraoperatively in 12 AS patients. T2 mapping (GraSE) was also performed. Myocardial native T1 with MOLLI and shMOLLI showed, firstly, an excellent discriminatory accuracy between health and disease [area under the curves (*P*-value): 0.94 (0.88–0.99); 0.87 (0.79–0.94); 0.61 (0.49–0.72)], secondly, relationship between histological CVF [native T1 MOLLI vs. shMOLLI vs. SASHA: $r = 0.582$ ($P = 0.027$), $r = 0.524$ ($P = 0.046$), $r = 0.443$ ($P = 0.150$)], and thirdly, with native T2 [$r = 0.628$($P < 0.001$), $r = 0.459$ ($P = 0.003$), $r = 0.211$ ($P = 0.083$)]. The respective relationships for extracellular volume fraction with CVF [$r = 0.489$ ($P = 0.044$), $r = 0.417$ (0.071), $r = 0.353$ ($P = 0.287$)] were significant for MOLLI, but not other sequences. In AS patients, native T2 was significantly higher compared to controls, and associated with levels of C-reactive protein and troponin.

Conclusion T1 mapping sequences differ in their bioequivalence for discrimination between health and disease as well as associations with diffuse myocardial fibrosis.

Keywords T1 mapping • MOLLI • shMOLLI • SASHA • collagen

* Corresponding author. Tel: +49-69-6301-86760; Fax: +49-69-6301-7983. E-mail: vppapers@icloud.com

Introduction

Myocardial T1 mapping provides a novel concept in quantitative tissue characterization, yielding a value, unlike relying on visually recognizable contrast differences. Thus, T1 mapping measurements can be used to relay biologically important properties in a quantitative manner, including the presence and severity of abnormal myocardium in many cardiac conditions. T1 indices have a potential to improve clinical diagnosis and risk stratification, particularly in conditions with diffuse myocardial involvement.[1] Despite the surge in evidence, the immediate clinical translation of these techniques is complicated by multiple variants of similar T1 mapping sequences. Each sequence and its modification yield different normal values and ranges, and show variable diagnostic performance in detection of abnormalities in human myocardium. Thus, each sequence will represent an individual diagnostic test, necessitating an individual clinical validation and standardization.[2]

T1 mapping sequences employed in myocardial characterization differ principally in magnetization preparation by either an inversion recovery (IR) or a saturation recovery (SR) prepulse (reviewed in Higgins *et al.*[3]) The many variants of these two approaches are further distinguished by different schemes of image acquisition (e.g. number of prepulses/images/pauses) and readout parameters [flip angle (FA), time delay, adiabatic prepulse, etc]. The sequence most commonly reported is based on the IR sequence MOdified Look-Locker (MOLLI). Following its original publication,[4] numerous MOLLI variants have been developed either to achieve shorter breath-holds[5,6] or greater T1 accuracy.[7] SR sequences benefit from a much shorter period of T1 relaxation following a SR preparation[8,9] and absence of history of magnetization of prior heartbeats, thus, shortening the overall acquisition time and improving the T1 accuracy, respectively. All T1 mapping methods are continuously and actively modified ('optimized') in terms of protocol parameters, scanner software versions, practical scanning methodology and methods of analysis, as well as manufacturer-specific implementations. In this study, we undertook sequence comparison of the 3 most commonly reported T1 mapping sequences—within the same individual—to examine their bioequivalence, or performance *in vivo*, in terms of diagnostic accuracy, relationships with histologically derived collagen volume fraction (CVF), and their T2 sensitivity by comparison with T2 mapping, in two model diseases of diffuse myocardial fibrosis; non-ischaemic dilative cardiomyopathy (NIDCM) and aortic stenosis (AS).

Methods

Consecutive patients from Guys and St. Thomas' and Kings College Hospitals were invited to participate in this study:

(1) Patients with NIDCM[10] ($n = 32$). Prior to their enrolment, the diagnosis was confirmed by cardiovascular magnetic resonance (CMR) on the basis of increased LV end-diastolic volume indexed to body surface area and reduced LV ejection fraction (EF < 50%) compared with published reference ranges normalized for age and sex.[11] Several of these subjects were included in our previous publications.[10,12,13]

(2) Patients with severe AS ($n = 25$) were identified from cardiology and cardiothoracic surgery outpatient clinics. AS was the leading valve problem based on Doppler echocardiographic demonstration of mean aortic valve pressure gradient >40 mmHg.[14]

(3) Asymptomatic and normotensive subjects ($n = 26$), taking no regular medication and with no significant medical history and normal CMR findings, including volumes and mass, served as controls.[12,15] Control subjects were recruited as a part of the parallel project into the normal values.[16] The subgroup was selected to provide an age-gender matched control group to the AS group.

Exclusion criteria for all subjects are detailed in supplementary material. Blood samples for haematocrit in AS patients were obtained contemporaneously at the time of the CMR procedure, whereas in patients with NIDCM these were based on the clinical blood tests.[10] Analysis of serological cardiac biomarkers, including N-terminal-pro brain natriuretic peptide (NT-BNP), type 1 procollagen C-terminal propeptide (PICP), high-sensitive (hs-) troponin and hs-C-reactive protein (CRP), was performed using commercial platforms. The study protocol was reviewed and approved by the local ethics committee, and written informed consent was obtained from all participants. All procedures were carried out in accordance with the Declaration of Helsinki (2013).

Image acquisition and analysis

All sequence parameters are detailed in the Supplementary material. Subjects underwent a routine clinical protocol for cardiac volumes and mass (with cine imaging) and tissue characterization with T1 mapping and late gadolinium enhancement (LGE) imaging using 3-Tesla MRI scanner equipped with advanced cardiac package and multi-transmit technology (Achieva, Philips Healthcare, Best, The Netherlands).[10,12,17] T1 mapping was performed using two MOLLI variants [the original MOLLI[4,10,12] and Shortened MOdified Look-Locker Inversion recovery (shMOLLI)[5]] and a SR variant, SAturation recovery single-SHot Acquisition (SASHA).[8] Sequences were acquired in random order (to avoid bias) in a single mid-ventricular short axis (SAX) slice, prior to and 15 minutes after intravenous administration of gadobutrol (0.2 mmol/kg per body weight, Gadovist®, Bayer Healthcare, Leverkusen, Germany). T2 mapping was performed in the same geometry using a hybrid gradient and spin echo GraSE sequence.

CMR analysis was performed using commercially available software (CVI42®, Circle Cardiovascular Imaging Ltd, Calgary, Canada) following standardized post-processing recommendations.[10,18] LGE images were visually examined for the presence of regional scar tissue in two phase-encoding directions and confirmed as positive if the visually positive regions had a SI > 4 standard deviations (SD) from normal regions.[17] Recovery rate of T1 and T2 relaxation for all sequences was measured conservatively within the septal myocardium, using PRIDE (Philips, Best, The Netherlands), as previously described and validated.[12,15] Areas of LGE were excluded from the mapping regions of interests (ROI). Care was taken to avoid contamination of myocardial signal with the blood pool. In addition to T1-values of native and post-contrast myocardium the gadolinium extracellular partition coefficient, the haematocrit-corrected extracellular volume fraction (ECV) was calculated.[19]

Myocardial biopsies and histological analysis

Several ($n \geq 3$ per person) intraoperative deep endomyocardial biopsy (EMB) samples were obtained in 12 AS patients using either biopsy forceps (Novatome, Scholten®) or direct surgical excision, as per choice of operator. EMBs were sampled from the mid-portion of the interventricular septum, avoiding the basal fibrotic membranous part. Sample preparation and analysis approach are described in supplementary material. Mean percent fibrosis (CVF), fibrosis heterogeneity (SD between fields), patient heterogeneity (interquartile range, IQR), and inter-observer coefficient of variation (CoV) are reported.

Table 1 Discrimination between health and disease

	Native T1		Post-contrast T1		ECV	
Controls vs. all patients	AUC (95% CI)	Sig (*P*-value)	AUC (95% CI)	Sig (*P*-value)	AUC (95% CI)	Sig (*P*-value)
MOLLI	0.94 (0.88–0.99)	<0.001	0.66 (0.54–0.77)	0.005	0.73 (0.64–0.83)	<0.001
ShMOLLI	0.87 (0.79–0.94)	<0.001	0.64 (0.52–0.75)	0.02	0.67 (0.58–0.79)	<0.001
SASHA	0.61 (0.49–0.72)	0.067	0.62 (0.50–0.73)	0.04	0.59 (0.46–0.72)	0.02
Native T2	0.81 (0.73–0.89)	<0.001	/	/	/	/

The comparative performance of each sequence to discriminate between health and disease controls and all patients) for native T1, post-contrast T1 and ECV, using ROC-curve analysis to derive AUC.

Statistical analysis

Statistical analysis was performed using SPSS software (SPSS Inc., Chicago, IL, USA, version 23.0). Normality of distributions was tested using Wilks-Shapiro statistic. Categorical data are expressed as percentages, and continuous variables as mean ± SD or median (interquartile range), as appropriate. Comparisons of the means between groups were performed using one way ANOVA (with Bonferroni *post hoc* tests for the differences from controls). Associations between variables were detected by bivariate linear regression analyses. Repeatability of measurements were assessed using intraclass-correlations (ICC). Receiver operating characteristic (ROC) curves was used in discrimination between health and disease. All values are reported as mean±SD and a *P*-value of less than 0.05 was considered statistically significant.

Results

A total of 83 subjects completed the imaging protocol with the 3 T1 mapping sequences. Subject characteristics and CMR results are presented in Supplementary data online, *Table S1*. Groups were similar for age, gender, heart rate and diastolic blood pressure, whereas the body-mass index and systolic BP were significantly higher in AS patients. Compared to controls, both patient groups had significantly higher indexed left ventricular (LV) volumes, LV mass, left atrial size, and lower LV and RV ejection fraction ($P < 0.05$ for all). All patients with AS has increased LV wall thickness ≥12 mm, measured in diastole. Non-ischaemic LGE was present in a total of 10 NIDCM (31%) and 5 AS (20%) patients. Patients had significantly higher mean E/e' on transthoracic echocardiography, as well as the levels of serological cardiac biomarkers.

Native T1 and ECV data show progressively larger imprecision and variation in normal controls from MOLLI to ShMOLLI to SASHA (see Supplementary data online, *Table S2*).[9,20] Compared with controls, native T1 and ECV were significantly higher in both patient groups for MOLLI and shMOLLI sequences ($P < 0.01$), whereas SASHA only revealed a significant difference between controls and patients with NIDCM. Post-contrast T1 values were significantly different for the MOLLI sequence but not shMOLLI or SASHA (*Table 2*). Native T2 was raised in NIDCM and AS patients, significantly in the latter group.

ROC curves in discrimination between health and disease (all patients) are presented in *Figure 1*, with respective area under the curves [(AUCs), 95% confidence interval (95% CI)] for all T1 mapping indices and sequences listed in *Table 1*. Native T1 for MOLLI showed the greatest ability to discriminate between health and disease [AUC: 0.94 (0.88–0.99), $P < 0.001$; comparisons of AUCs: MOLLI vs. shMOLLI, SASHA and T2: $P = 0.064$, $P < 0.001$, $P = 0.01$, respectively]. Native T2 also showed a strong ability to differentiate between health and disease [AUC: 0.81 (0.73–0.89), $P < 0.001$]. Native T1 by MOLLI was an independent discriminator between health and disease ($\chi^2 = 52$, $P < 0.001$).

Results of myocardial histology and associations with T1 mapping indices are presented in *Table 2* (*Figures 2* and *3*). Procedurally, all EMBs were uneventful ($n = 12$). The mean histological CVF was 25.6% (intersubject IQR 10.1–43.2%, SD 18.6). There was an excellent agreement between the two observers ($r = 0.95$, $P < 0.01$; MD ± SD = 5.9 ± 4.6). Correlations between CVF with all T1 mapping indices for various sequences are included in *Table 2* (*Figure 4*). There was moderate significant association for native T1 with MOLLI and shMOLLI, whereas correlation with SASHA was not significant. For ECV only MOLLI showed a significant association. Native T2 showed a mild but not significant association with CVF ($r = 0.271$, $P = 0.24$). *Table 3* summarizes the correlations with serological markers for all T1 mapping indices in AS and NIDCM patients. Native T1 with MOLLI and shMOLLI, post-contrast T1 with MOLLI, and native T2 showed significant associations with N-terminal prohormone of brain natriuretic peptide (NT-proBNP), hs-troponin and CRP, but not PICP. Repeatability of measurements (ICCs) are reported in Supplementary Material.

Discussion

We demonstrate that T1 mapping sequences differ considerably in their performance in myocardial tissue characterization, as evidenced by differential ability to discriminate between health and disease and by diverse associations with myocardial CVF and T2 mapping. More specifically, our findings reveal that native T1 using MOLLI sequences show an excellent diagnostic performance in detecting the differences in myocardium between controls and patients. Myocardial T1 mapping with MOLLI sequences showed the strongest relationship with histologically derived CVF and with T2 mapping.

A number of previous studies reported on associations with tissue collagen content or discrimination between health and disease (summarized in *Figure 4*, modified from[1]) We expand these findings by comprehensive and standardized intraindividual acquisition of more than one sequence and analysis of all T1 indices. Compared with a previous reports we found similar associations for native T1 with CVF for shMOLLI.[22] For MOLLI, previous studies reported diverse

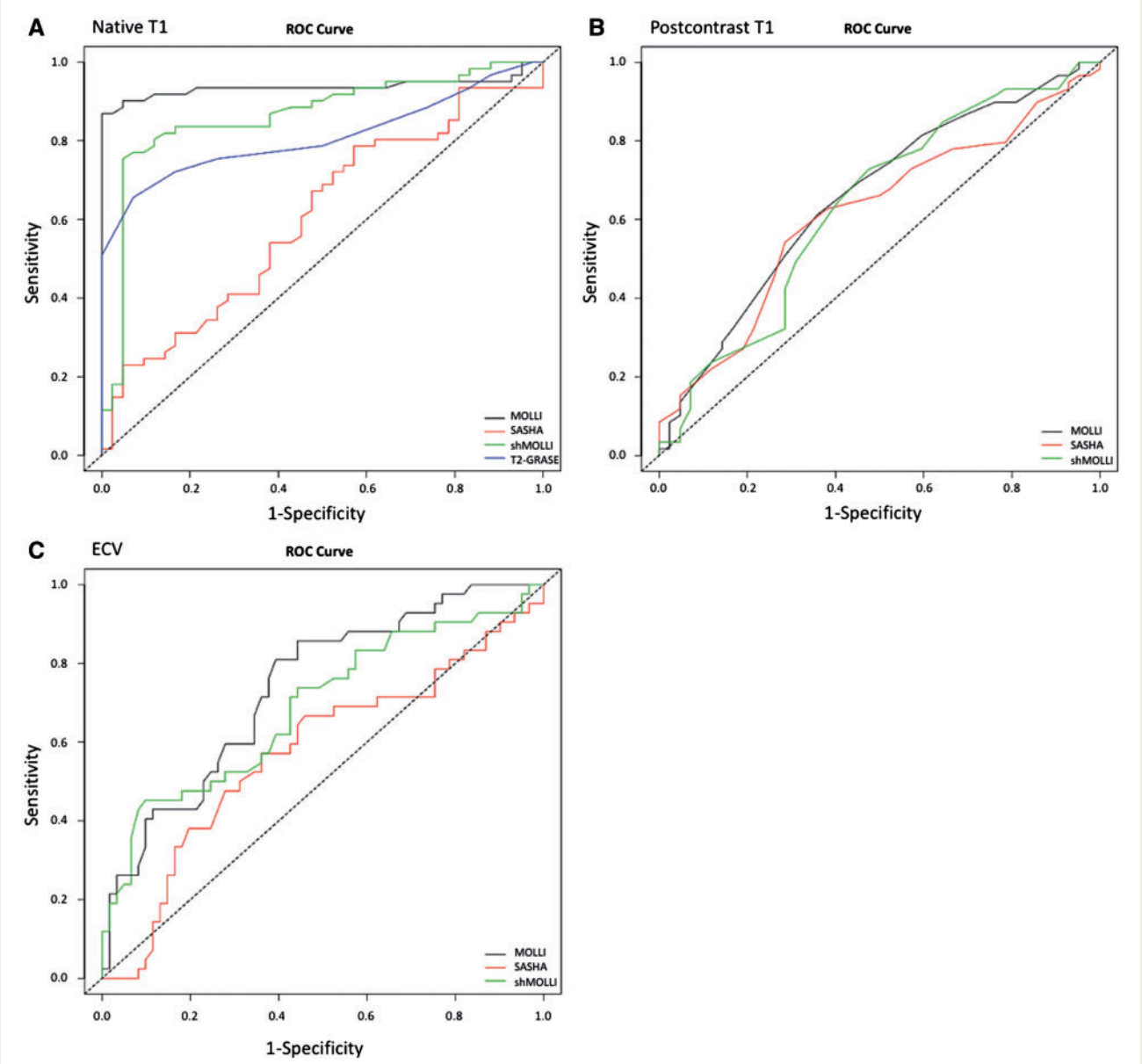

Figures I Native T1 (*A*), post-contrast T1 (*B*), and ECV (*C*) in discrimination between health and disease for three sequences in all patients against healthy controls using ROC curve analysis.

associations for native T1 and CVF ranging between 0.15 and 0.77,[1] and our results add to the favourable side of that range. Associations for ECV, however, were much lower for both shMOLLI[23,24] and MOLLI.[34] Several possible reasons may explain these findings, especially the type of sequences, given the implementation and optimization of shMOLLI and SASHA on a new vendor platform. The use of motion correction, types of post-processing softwares and approaches, the type and dose of gadolinium contrast, histological dyes, reading methods, etc., may all influence the measurements. The severity of myocardial damage can vary considerably between the patients included at the different sites; which in such small samples may be a major factor. Although the biopsies were performed during open-heart surgery, inclusion of replacement fibrosis during the tissue sampling is difficult to control. This complication of human EMBs in introducing the sampling errors is also well recognized.[32,35] We strived for exclusion of LGE given our strong focus on to the diffuse myocardial disease, yet, we acknowledge that definition of 'diffuse' will depend on the spatial resolution of the LGE technique allowing to differentiate localized patterns of fibrosis from the remaining tissue, unlike averaging them within one voxel. The post-processing approach in studies that have not accounted for the regional variations or inadvertent inclusion of blood partial volume in myocardial T1 values,[30,31,36] may reveal different results than in the studies using conservative septal ROI.[15,26,37] The discriminatory power of ECV values may also suffer from dependency on two separate measurements. Finally, the association between CVF and ECV by

Table 2 Summary of studies reporting on association between CVF and T1 mapping indices modified and adapted from[1] (with permission)

Collagen volume fraction%	Sequence	Pearson *r* (Sig)	No. of patients (cardiac disease)	GCAs (dose and type)	T1 Index	Histological staining
Aortic stenosis						
Flett *et al.*[21]	GRE-IR	0.94 (0.001)	18	(0.2 mmol/kg gadoterate meglumine)	ECV (EQ)	Picrosirius red
Bull *et al.*[22]	shMOLLI	0.655 (0.002)	19		Native T1	Picrosirius red
Fontana *et al.*[23]	GRE-IR	0.78 (<0.01)	18	(0.2 mmol/kg gadoterate meglumine)	ECV (EQ)	Picrosirius red
	shMOLLI	0.83 (<0.01)				
White *et al.*[24]	shMOLLI	0.83 (<0.01)	18	(0.2 mmol/kg gadoterate meglumine)	ECV (bolus)	Picrosirius red
		0.84 (<0.01)			ECV (EQ)	
de Meester de Ravenstein *et al.*[25]	MOLLI 3(3)3(3)5 (FA35°)	-0.15 (0.64)	12	(0.2 mmol/kg gadobutrol)	Native T1	Picrosirius red
		-0.64 (0.024)			Post-contrast T1	
		0.91 (0.001)			ECV	
Lee *et al.*[26]	MOLLI 3(3)3(3)5(FA35°)	0.77 (<0.01)	10		Native T1	Picrosirius red
Child	*MOLLI 3(2)3(2)5(FA50°)*	*0.582 (0.027)*	*12*	*(0.2 mmol/kg gadobutrol)*	*Native T1*	*Masson-trichrome*
		−0.47 (0.065)			*Post-contrast T1*	
		0.498 (0.044)			*ECV*	
	shMOLLI	*0.524 (0.046)*			*Native T1*	
		−0.45 (0.140)			*Post-contrast T1*	
		0.417 (0.071)			*ECV*	
	SASHA	*0.442 (0.150)*			*Native T1*	
		−0.27 (0.411)			*Post-contrast T1*	
		0.353 (0.287)			*ECV*	
Heart failure						
Iles *et al.*[27]	VAST	-0.7 (0.03)	9 (IHD)	(0.2 mmol/kg gadopentetate dimeglumine)	Post-contrast T1	Picrosirius red
Sibley *et al.*[28]	Look-Locker	-0.57 (<0.001)	47 (NICMs)	(0.2 mmol/kg gadodiamide)	Post-contrast T1	Masson trichrome
Mascherbauer *et al.*[29]	GRE-IR	-0.98 (<0.01)	9 (HFpPEF)	(0.2 mmol/kg gadobutrol)	Post-contrast T1	Masson Trichrome/ Congo-red
Miller *et al.*[30]	MOLLI 3(3)3(3)5(FA 35°)	0.199 (0.437)	6 (IHD)	(0.2 mmol/kg (gadopentetate dimeglumine)	Native T1	Picrosirius red
		-0.21 (0.69)			Post-contrast T1	
		0.945 (0.004)			ECV (bolus)	
Aus dem Siepen *et al.*[31]	MOLLI 3(3)3(3)5(FA 35°)	0.85 (0.01)	45 (DCM)	(0.2 mmol/kg gadopentetate dimeglumine)	ECV (bolus)	Acid Fuchsin Orange-G
Iles *et al.*[32]	VAST	0.73 (<0.001)	4 (1 IHD, 3 DCM)	(0.2 mmol/kg gadopentetate dimeglumine)	LGE	Masson Trichrome
		-0.64 (0.002)			Post-contrast T1	
Kammerlander *et al.*[33]	MOLLI 5(3)3 (FA 35°) for native acquisition MOLLI 4(1)3(1)2(FA 35°) for post-contrast acquisition	0.493 (<0.002)	36 (mixed group)	(0.1 mmol/kg of gadobutrol)	ECV (bolus)	Tissue FAXS
Hypertrophic cardiomyopathy						
Flett *et al.*[21]	GRE-IR	R^2 = 0.62(0.08), Tau = 0.52	8	(0.2 mmol/kg gadoterate meglumine)	ECV	Picrosirius red

Continued

Table 2 *Continued*

Collagen volume fraction%	Sequence	Pearson *r* (Sig)	No. of patients (cardiac disease)	GCAs (dose and type)	T1 Index	Histological staining
Iles *et al.*[32]	VAST	-0.71 (0.01)	8	(0.2 mmol/kg gadopentetate dimeglumine)	Post-contrast T1	Masson-trichrome

Types of sequences and a staining method used, as well as numbers of patients included, is also reported., GCAs, gadolinium contrast agents, IHD, ischaemic heart disease; HFpEF, heart failure with preserved ejection fraction; NICM, non-ischaemic cardiomyopathy; GRE-IR, gradient echo-inversion recovery; VAST, variable sampling of k-space in time.

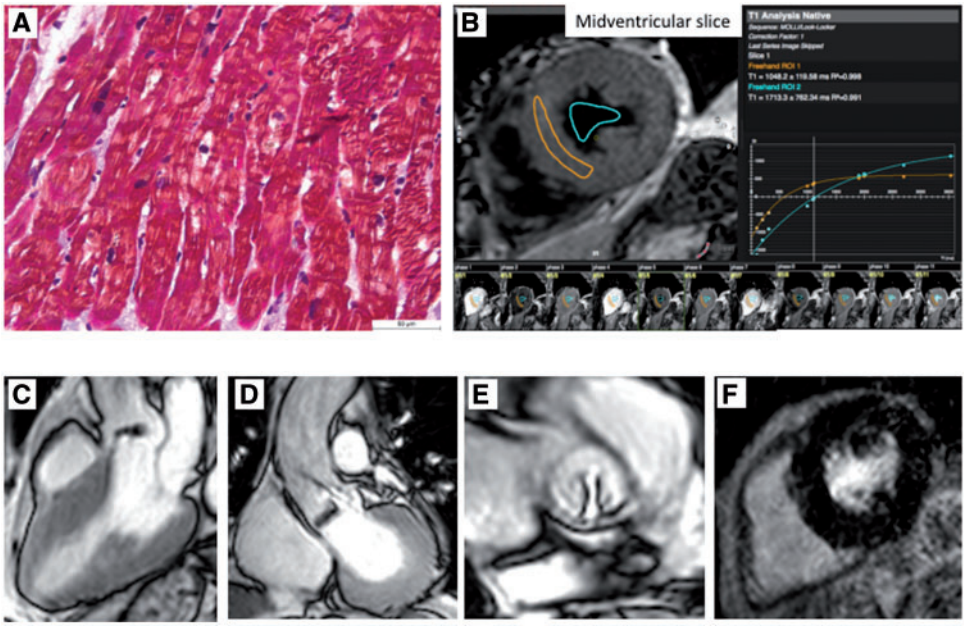

Figures 2 Representative images of patients with AS—Case 1. (*A*) Histological analysis with Mason Trichrome reveals mild-moderate interstitial fibrosis (CVF = 16%). MOLLI measurement reveal native T1 1068 ms (*B*) and ECV = 26%. Cine imaging in mid-systole: 3-chamber (*C*), LVOT (*D*) view and AV valve view, revealing significantly reduced AV opening (AV area by planimetry 0.56 cm^2). There is no evidence of late gadolinium enhancement (*F*). NTproBNP 634 ng/L.

MOLLI found in the present study ($r = 0.498$) compares favourably to the result using tissue FAXS technology[33] ($r = 0.493$).

A further interesting finding is the correlation of T1 indices with T2 mapping. This observation communicates an important influence of transverse relaxation, which appears to be captured within the myocardial T1 mapping, consistent with previous reports highlighting the proneness of MOLLI variants to the T2-related errors.[20] The effect of magnetization transfer (MT) in MOLLI variants, may be resulting from acquisition of multiple images after each preparation pulse.[3,20,38] The difference in FA between implementation of our MOLLI sequence[4,10,12] vs. ShMOLLI[5] (50° vs. 35°) explains the greater SNR and possibly also the more pronounced T2 and MT effects for MOLLI. Whereas the development of techniques, which are highly accurate for T1 with minimal contamination by T2 or MT or other effects is important for post-contrast T1 acquisitions (i.e. 'true T1 mapping'), the advantages of the T2-proneness for native T1 mapping—high precision and diagnostic accuracy, yielding higher sensitivity to myocardial pathophysiology, can from the clinical standpoint not be overlooked. Clearly, further research is warranted to elucidate these clinically relevant effects.

Lastly, we reveal for the first time that in AS, myocardial native T2 is significantly raised. As it is not significantly associated with myocardial collagen content, it may suggest myocardial oedema.[39–42] A body of evidence substantiates the role of inflammatory cellular and extracellular processes in myocardial plasticity and remodelling in response to increased LV wall stress,[43,44] including a reactivation of hypertrophic foetal gene programme with phenotypical expression of natriuretic peptides, such as NT-pro BNP, which was also found elevated in the present study.[44–47] Increased hs-troponin and CRP levels and relationship with T1 and T2 indices in AS patients may lend

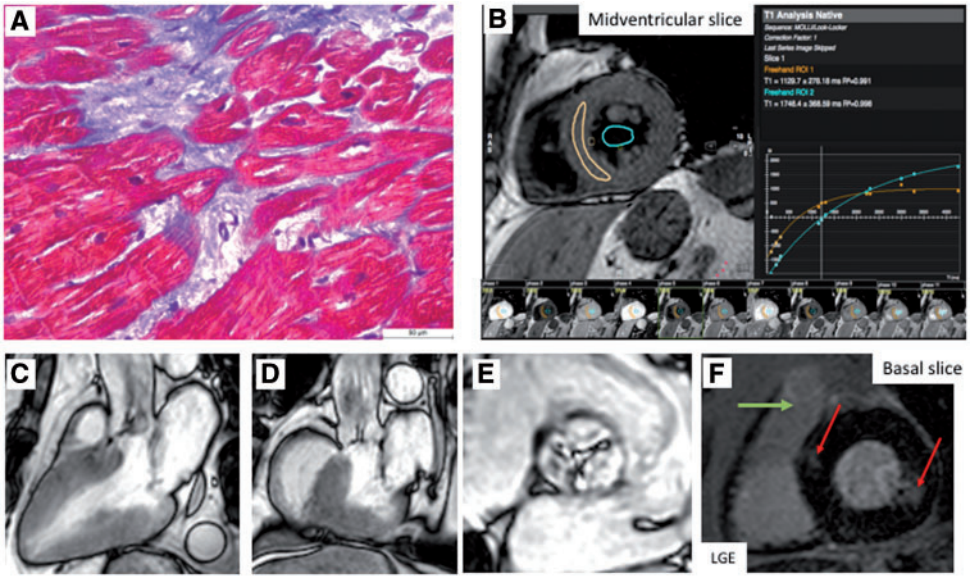

Figures 3 Representative images of patients with AS—Case 2. (*A*) Histological analysis with Mason Trichrome reveals considerable myocardial fibrosis (CVF 37%). MOLLI measurement in mid-ventricular SAX slice show native T1 1130 ms (*B*) and ECV 32%. Cine imaging in mid-systole: 3-chamber (*C*), LVOT (*D*) view and AV valve view, reduced AV opening (AV area by planimetry 0.37 cm^2). Evidence of non-ischaemic late gadolinium enhancement in basal anteroseptal and inferolateral segments—red arrows (green arrow points to the basal RV structures, including RV outflow tract and pulmonary valve) (*F*). NTproBNP 1381 ng/L.

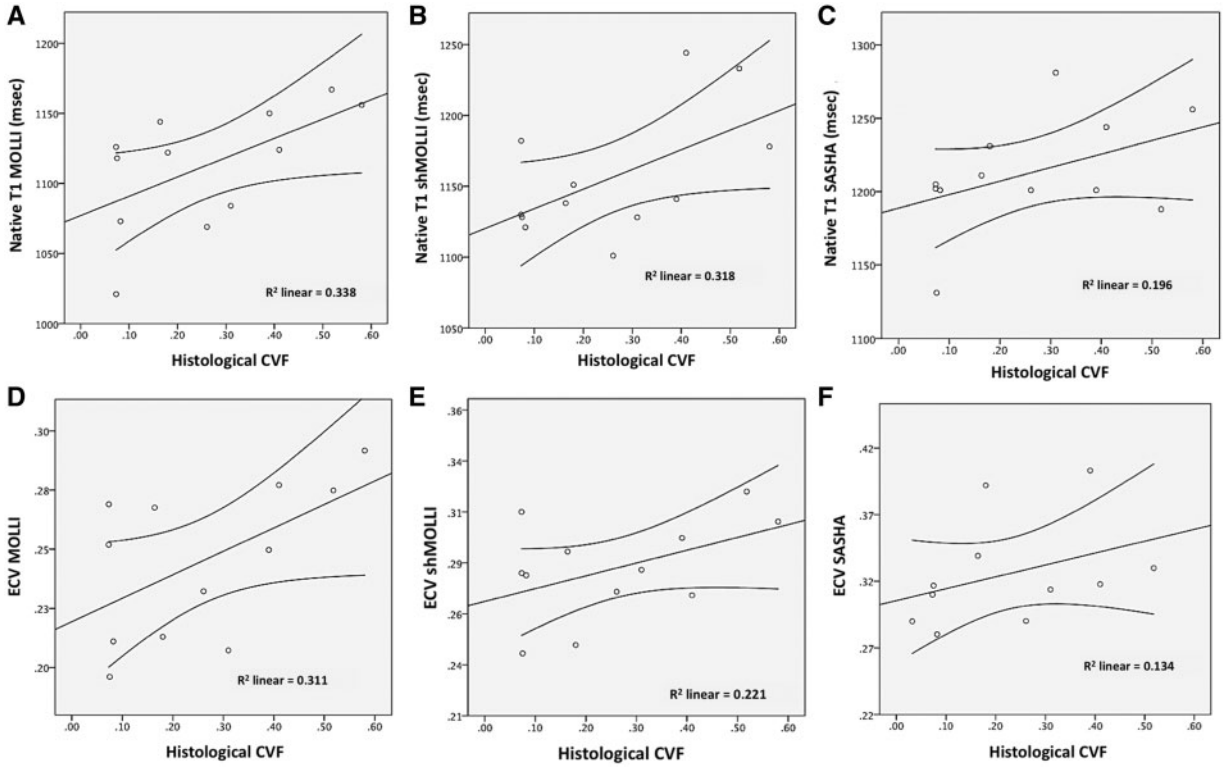

Figure 4 Correlations between T1 mapping measurements and histologically derived CVF—native T1 (*A*–*C*) and ECV (*D*–*F*).

Table 3 Correlations between T1 and T2 mapping indices and serological markers in AS patients ($n = 25$) using Pearson correlation (r-statistic)

	AS patients ($n = 25$)					NIDCM patients ($n = 34$)			
	T2 mapping (ms)	NT-proBNP	hs-Troponin	hs-CRP	PICP	NT-proBNP	hs-Troponin	hs-CRP	PICP
MOLLI									
Native T1 (ms)	0.628**	0.404*	0.324*	0.550**	0.284	0.441*	0.145	0.362*	0.316
Post-contrast T1 (ms)	-0.22	-0.470*	-0.334	-0.351*	-0.091	-0.328	-0.122	-0.291	-0.172
ECV (%)	0.248*	0.327	0.272	0.216	0.070	0.315	0.171	0.226	0.231
ShMOLLI									
Native T1 (ms)	0.459**	0.379*	0.217	0.409*	0.32	0.427*	0.160	0.350*	0.293
Post-contrast T1 (ms)	-0.16	-0.311	-0.201	-0.308	-0.19	-0.247	-0.114	-0.314	-0.189
ECV (%)	0.236*	0.234	0.195	0.142	0.068	0.285	0.125	0.164	0.193
SASHA									
Native T1 (ms)	0.211	0.095	0.099	0.213	0.083	0.136	0.083	0.291	0.233
Post-contrast T1 (ms)	0.027	-0.055	-0.025	-0.139	-0.069	-0.049	-0.053	-0.129	-0.061
ECV (%)	0.471	0.032	0.112	0.217	0.134	0.047	0.193	0.116	0.053
Native T2		0.414*	0.366*	0.382*	0.118	0.362*	0.162	0.351*	0.148

P-value of < 0.05 was statistically significant; * $P < 0.05$, ** $P < 0.01$.

a further support to the notion that myocardial oedema, alongside interstitial fibrosis,[48] represents a detectable process in extracellular matrix remodelling in hypertrophic cardiac conditions.

Study limitations

A few limitations apply. This is a single centre, single-vendor and single field-strength comparison study in a sample size, which is based on the previous studies using the identical MOLLI sequence.[12] EMBs were performed within the conservative constraints of ethical approval for an invasive procedure performed purely for research purposes. We strived to include a sufficient number of patients required to achieve a significant correlation for native T1 with MOLLI sequence (type I error; $\alpha < 0.05$) (Type II error; $\beta = 0.8$; $n = 8$), which was also reconfirmed by a *post hoc* analysis. However, the sample size was not powered to inform on the superiority of correlations between the mapping techniques. The study-design, i.e. head-to-head comparison, and standardized approach to imaging and histology obtained within the same subject, eliminates several important methodological biases, which make comparisons between studies using single techniques difficult. We believe that our results provide a useful guide to the type of much needed evidence, required to support an informed clinical use of T1 mapping sequences.

Conclusions

We demonstrate that T1 mapping indices and sequences differ in their bioequivalence for detection of abnormal myocardium, which is characterized by diffuse interstitial myocardial fibrosis. Native T1 with MOLLI sequences provides the strongest discriminatory accuracy in characterization of human myocardium.

Supplementary data

Supplementary data are available at *European Heart Journal - Cardiovascular Imaging* online.

Acknowledgments

We would like to acknowledge the support of Cardiology and Cardiothoracic Surgery departments at Guy's and St Thomas' and King's College Hospitals NHST Trusts; cardiac radiographers for obtaining the high-quality imaging studies; Philips Clinical Scientists for support: David M. Higgins, PhD; Bernhard Schnackenburg, PhD; Christian Stehning, PhD; Eltjo Haselhoff, PhD.

Funding

Department of Health through the National Institute for Health Research (NIHR) comprehensive Biomedical Research Centre award to Guy's & St. Thomas' NHS Foundation Trust in partnership with King's College London and King's College Hospital NHS Foundation Trust. Histological comparisons in aortic stenosis patients were supported by Medical Research Council - Confidence in Concept 2012' administered through King's Health Partners project grant (MRJBACR). N.C. was funded by an educational grant from St. Jude Medical. VP, EN, SD, MR-M are supported by the German Centre of Cardiovascular Research (DZHK).

Conflict of interest: None declared.

References

1. Puntmann VO, Peker E, Chandrashekhar Y, Nagel E. T1 mapping in characterizing myocardial disease. *Circ Res* 2016;**119**:277–99.
2. Biomarkers Definitions Working Group. Biomarkers and surrogate endpoints: preferred definitions and conceptual framework. *Clin Pharmacol Ther* 2001;**69**:89–95.
3. Higgins DM, Moon JC. Review of T1 mapping methods: comparative effectiveness including reproducibility issues. *Curr Cardiovasc Imaging Rep* 2014;**7**:9252.
4. Messroghli DR, Radjenovic A, Kozerke S, Higgins DM, Sivananthan MU, Ridgway JP. Modified Look-Locker inversion recovery (MOLLI) for high-resolutionT1 mapping of the heart. *Magn Reson Med* 2004;**52**:141–6.

5. Piechnik SK, Ferreira VM, Dall'Armellina E, Cochlin LE, Greiser A, Neubauer S *et al*. Shortened Modified Look-Locker Inversion recovery (ShMOLLI) for clinical myocardial T1-mapping at 1.5 and 3 T within a 9 heartbeat breathhold. *J Cardiovasc Magn Reson* 2010;**12**:69.
6. Lee JJ, Liu S, Nacif MS, Ugander M, Han J, Kawel N *et al*. Myocardial T1 and extracellular volume fraction mapping at 3 tesla. *J Cardiovasc Magn Reson* 2011; **13**:75.
7. Radunski UK, Lund GK, Stehning C, Schnackenburg B, Bohnen S, Adam G *et al*. CMR in patients with severe myocarditis. *JACC Cardiovasc Imaging* 2014;**7**:667–75.
8. Chow K, Flewitt JA, Green JD, Pagano JJ, Friedrich MG, Thompson RB. Saturation recovery single-shot acquisition (SASHA) for myocardial T1mapping. *Magn Reson Med* 2014;**71**:2082–95.
9. Roujol S, Weingärtner S, Foppa M, Chow K, Kawaji K, Ngo LH *et al*. Accuracy, precision, and reproducibility of four T1 mapping sequences: a head-to-head comparison of MOLLI, ShMOLLI, SASHA, and SAPPHIRE. *Radiology* 2014;**272**: 683–9.
10. Puntmann VO, Carr-White G, Jabbour A, Yu C-Y, Gebker R, Kelle S *et al*. T1-mapping and outcome in nonischemic cardiomyopathy. *JACC Cardiovasc Imaging* 2016;**9**:40–50.
11. Natori S, Lai S, Finn JP, Gomes AS, Hundley WG, Jerosch-Herold M *et al*. Cardiovascular function in multi-ethnic study of atherosclerosis: normal values by age, sex, and ethnicity. *AJR Am J Roentgenol* 2006;**186**:S357–65.
12. Puntmann VO, Voigt T, Chen Z, Mayr M, Karim R, Rhode K *et al*. Native T1 mapping in differentiation of normal myocardium from diffuse disease in hypertrophic and dilated cardiomyopathy. *JACC Cardiovasc Imaging* 2013;**6**:475–84.
13. Puntmann VO, Arroyo Ucar E, Hinojar Baydes R, Ngah NB, Kuo YS, Dabir D *et al*. Aortic stiffness and interstitial myocardial fibrosis by native T1 are independently associated with left ventricular remodeling in patients with dilated cardiomyopathy. *Hypertension* 2014;**64**:762–8.
14. Authors/Task Force members, Vahanian A, Alfieri O, Andreotti F, Antunes MJ, Baron-Esquivias G, Baumgartner H *et al*. Guidelines on the management of valvular heart disease (version 2012): the Joint Task Force on the Management of Valvular Heart Disease of the European Society of Cardiology (ESC) and the European Association for Cardio-Thoracic Surgery (EACTS). *Eur Heart J* 2012; **33**:2451–96.
15. Rogers T, Dabir D, Mahmoud I, Voigt T, Schaeffter T, Nagel E *et al*. Standardization of T1 measurements with MOLLI in differentiation between health and disease—the ConSept study. *J Cardiovasc Magn Reson* 2013;**15**:78.
16. Dabir D, Child N, Kalra A, Rogers T, Gebker R, Jabbour A *et al*. Reference values for healthy human myocardium using a T1 mapping methodology: results from the International T1 multicenter cardiovascular magnetic resonance study. *J Cardiovasc Magn Reson* 2014;**16**:34.
17. Kramer CM, Barkhausen J, Flamm SD, Kim RJ, Nagel E; Society for Cardiovascular Magnetic Resonance. Standardized cardiovascular magnetic resonance (CMR) protocols 2013 update. *J Cardiovasc Magn Reson* 2013;**15**:91.
18. Schulz-Menger J, Bluemke DA, Bremerich J, Flamm SD, Fogel MA, Friedrich MG *et al*. Standardized image interpretation and post processing in cardiovascular magnetic resonance: Society for Cardiovascular Magnetic Resonance (SCMR) Board of Trustees Task Force on Standardized Post Processing. *J Cardiovasc Magn Reson* 2013;**15**:35.
19. Jerosch-Herold M, Sheridan DC, Kushner JD, Nauman D, Burgess D, Dutton D *et al*. Cardiac magnetic resonance imaging of myocardial contrast uptake and blood flow in patients affected with idiopathic or familial dilated cardiomyopathy. *Am J Physiol Heart Circ Physiol* 2008;**295**:H1234–42.
20. Kellman P, Hansen MS. T1-mapping in the heart: accuracy and precision. *J Cardiovasc Magn Reson* 2014;**16**:2.
21. Flett AS, Hayward MP, Ashworth MT, Hansen MS, Taylor AM, Elliott PM *et al*. Equilibrium contrast cardiovascular magnetic resonance for the measurement of diffuse myocardial fibrosis: preliminary validation in humans. *Circulation* 2010;**122**: 138–44.
22. Bull S, White SK, Piechnik SK, Flett AS, Ferreira VM, Loudon M *et al*. Human non-contrast T1 values and correlation with histology in diffuse fibrosis. *Heart* 2013;**99**:932–7.
23. Fontana M, White SK, Banypersad SM, Sado DM, Maestrini V, Flett AS *et al*. Comparison of T1 mapping techniques for ECV quantification. Histological validation and reproducibility of ShMOLLI versus multibreath-hold T1 quantification equilibrium contrast CMR. *J Cardiovasc Magn Reson* 2012;**14**:88.
24. White SK, Sado DM, Fontana M, Banypersad SM, Maestrini V, Flett AS *et al*. T1 mapping for myocardial extracellular volume measurement by CMR. *JACC Cardiovasc Imaging* 2013;**6**:955–62.
25. de Meester de Ravenstein C, Bouzin C, Lazam S, Boulif J, Amzulescu M, Melchior J *et al*. Histological validation of measurement of diffuse interstitial myocardial fibrosis by myocardial extravascular volume fraction from Modified Look-Locker imaging (MOLLI) T1 mapping at 3 T. *J Cardiovasc Magn Reson* 2015;**17**:1268.
26. Lee S-P, Lee W, Lee JM, Park E-A, Kim H-K, Kim Y-J *et al*. Assessment of diffuse myocardial fibrosis by using MR imaging in asymptomatic patients with aortic stenosis. *Radiology* 2015;**274**:359–69.
27. Iles L, Pfluger H, Phrommintikul A, Cherayath J, Aksit P, Gupta SN *et al*. Evaluation of diffuse myocardial fibrosis in heart failure with cardiac magnetic resonance contrast-enhanced T1 mapping. *J Am Coll Cardiol* 2008;**52**:1574–80.
28. Sibley CT, Noureldin RA, Gai N, Nacif MS, Liu S, Turkbey EB *et al*. T1 mapping in cardiomyopathy at cardiac MR: comparison with endomyocardial biopsy. *Radiology* 2012;**265**:724–32.
29. Mascherbauer J, Marzluf BA, Tufaro C, Pfaffenberger S, Graf A, Wexberg P *et al*. Cardiac magnetic resonance postcontrast T1 time is associated with outcome in patients with heart failure and preserved ejection fraction. *Circ Cardiovasc Imaging* 2013;**6**:1056–65.
30. Miller CA, Naish JH, Bishop P, Coutts G, Clark D, Zhao S *et al*. Comprehensive validation of cardiovascular magnetic resonance techniques for the assessment of myocardial extracellular volume. *Circ Cardiovasc Imaging* 2013;**6**:373–83.
31. Aus Dem Siepen F, Buss SJ, Messroghli D, Andre F, Lossnitzer D, Seitz S *et al*. T1 mapping in dilated cardiomyopathy with cardiac magnetic resonance: quantification of diffuse myocardial fibrosis and comparison with endomyocardial biopsy. *Eur Heart J Cardiovasc Imaging* 2015;**16**:210–6.
32. Iles LM, Ellims AH, Llewellyn H, Hare JL, Kaye DM, McLean CA *et al*. Histological validation of cardiac magnetic resonance analysis of regional and diffuse interstitial myocardial fibrosis. *Eur Heart J Cardiovasc Imaging* 2015;**16**:14–22.
33. Kammerlander AA, Marzluf BA, Zotter-Tufaro C, Aschauer S, Duca F, Bachmann A *et al*. T1 mapping by CMR imaging. *JACC Cardiovasc Imaging* 2016;**9**:14–23.
34. Schelbert EB, Sabbah HN, Butler J, Gheorghiade M. Employing extracellular volume cardiovascular magnetic resonance measures of myocardial fibrosis to foster novel therapeutics. *Circ Cardiovasc Imaging* 2017;**10**:e005619.
35. Cooper LT, Baughman KL, Feldman AM, Frustaci A, Jessup M, Kuhl U *et al*. The role of endomyocardial biopsy in the management of cardiovascular disease: a scientific statement from the American Heart Association, the American College of Cardiology, and the European Society of Cardiology. *Circulation* 2007;**116**: 2216–33.
36. Chin CWL, Semple S, Malley T, White AC, Mirsadraee S, Weale PJ *et al*. Optimization and comparison of myocardial T1 techniques at 3T in patients with aortic stenosis. *Eur Heart J Cardiovasc Imaging* 2014;**15**:556–65.
37. Child N, Yap ML, Dabir D, Rogers T, Suna G, Sandhu B *et al*. T1 values by conservative septal postprocessing approach are superior in relating to the interstitial myocardial fibrosis: findings from patients with severe aortic stenosis. *J Cardiovasc Magn Reson* 2015;**17**:P49.
38. Robson MD, Piechnik SK, Tunnicliffe EM, Neubauer S. T1measurements in the human myocardium: the effects of magnetization transfer on the SASHA and MOLLI sequences. *Magn Reson Med* 2013;**70**:664–70.
39. Hinojar R, Foote L, Arroyo Ucar E, Jackson T, Jabbour A, Yu C-Y *et al*. Native T1 in discrimination of acute and convalescent stages in patients with clinical diagnosis of myocarditis. *JACC Cardiovasc Imaging* 2015;**8**:37–46.
40. Lurz P, Luecke C, Eitel I, Föhrenbach F, Frank C, Grothoff M *et al*. Comprehensive cardiac magnetic resonance imaging in patients with suspected myocarditis. *J Am Coll Cardiol* 2016;**67**:1800–11.
41. Fernández-Jiménez R, García-Prieto J, Sánchez-González J, Agüero J, López-Martín GJ, Galán-Arriola C *et al*. Pathophysiology underlying the bimodal edema phenomenon after myocardial ischemia/reperfusion. *J Am Coll Cardiol* 2015;**66**: 816–28.
42. Ugander M, Bagi PS, Oki AJ, Chen B, Hsu L-Y, Aletras AH *et al*. Myocardial edema as detected by pre-contrast T1 and T2 CMR delineates area at risk associated with acute myocardial infarction. *JACC Cardiovasc Imaging* 2012;**5**:596–603.
43. Hill JA, Olson EN. Cardiac plasticity. *N Engl J Med* 2008;**358**:1370–80.
44. Westermann D, Lindner D, Kasner M, Zietsch C, Savvatis K, Escher F *et al*. Cardiac inflammation contributes to changes in the extracellular matrix in patients with heart failure and normal ejection fraction. *Circ Heart Fail* 2011;**4**: 44–52.
45. van Heerebeek L, Franssen CPM, Hamdani N, Verheugt FWA, Somsen GA, Paulus WJ. Molecular and cellular basis for diastolic dysfunction. *Curr Heart Fail Rep* 2012;**9**:293–302.
46. Frey N, Olson EN, Hill JA. Mechanisms of stress-induced cardiac hypertrophy. In: *Muscle*. Elsevier; 2012. p481–94.
47. Lazzeroni D, Rimoldi O, Camici PG. From left ventricular hypertrophy to dysfunction and failure. *Circ J* 2016;**80**:555–64.
48. Dimmeler S, Zeiher AM. Netting insights into fibrosis. *N Engl J Med* 2017;**376**: 1475–7.